Atmos. Chem. Phys. Discuss., 9, 10487–10511, 2009
www.atmos-chem-phys-discuss.net/9/10487/2009/


**Atmospheric Chemistry and Physics Discussions**

This discussion paper is/has been under review for the journal *Atmospheric Chemistry and Physics (ACP)*. Please refer to the corresponding final paper in *ACP* if available.

# Satellite measurements of formaldehyde from shipping emissions

**T. Marbach[1], S. Beirle[1], U. Platt[2], P. Hoor[1], F. Wittrock[3], A. Richter[3], M. Vrekoussis[3], M. Grzegorski[1], J. P. Burrows[3,4], and T. Wagner[1]**

[1]Max Planck Institute for Chemistry, Mainz, Germany
[2]Institute of Environmental Physics, Heidelberg, Germany
[3]Institute of Environmental Physics, Bremen, Germany
[4]Center for Ecology and Hydrology, Wallingford, UK

Received: 18 March 2009 – Accepted: 16 April 2009 – Published: 30 April 2009

Correspondence to: T. Marbach (marbach@mpch-mainz.mpg.de)

Published by Copernicus Publications on behalf of the European Geosciences Union.



**Abstract**

International shipping is recognized as a pollution source of growing importance, in particular in the remote marine boundary layer. Nitrogen dioxide originating from ship emissions has previously been detected in satellite measurements. This study presents the first satellite measurements of formaldehyde (HCHO) linked to shipping emissions as derived from observations made by the Global Ozone Monitoring Experiment (GOME) instrument.

We analyzed enhanced HCHO tropospheric columns from shipping emissions over the Indian Ocean between Sri Lanka and Sumatra. This region offers good conditions in term of plume detection with the GOME instrument as all ship tracks follow a single narrow track in the same east-west direction as used for the GOME pixel scanning. The HCHO signal alone is weak but could be clearly seen in the high-pass filtered data. The line of enhanced HCHO in the Indian Ocean as seen in the 7-year composite of cloud free GOME observations clearly coincides with the distinct ship track corridor from Sri Lanka to Indonesia. The observed mean HCHO column enhancement over this shipping route is about $2.0\times10^{15}$ molec/cm$^2$.

The observed HCHO pattern also agrees qualitatively well with results from the coupled earth system model ECHAM5/MESSy applied to atmospheric chemistry (EMAC). However, the modelled HCHO values over the ship corridor are two times lower than in the GOME high-pass filtered data. This might indicate that the used emission inventories are too low and/or that the in-plume chemistry taking place in the narrow path of the shipping lanes are not well represented at the rather coarse model resolution.

## 1 Introduction

Formaldehyde (HCHO) is an important indicator of tropospheric volatile organic compounds (VOCs) emissions from various sources as it is a principal intermediate in the oxidation of VOCs in the troposphere. The global atmospheric HCHO “background”

originates mainly from the oxidation of methane ($CH_4$) by the hydroxyl radical (OH) in the troposphere. Additional primary HCHO sources, locally emanate from biomass burning and fossil fuel combustion (Anderson et al., 1996). Moreover, HCHO is formed in the atmosphere as an intermediate in the photochemical oxidation of non-methane hydrocarbons from biogenic or anthropogenic sources (mainly isoprene and alkenes Meller and Moortgat, 2000). The major known sinks of HCHO are photolysis and reaction with OH or/and wet deposition. Due to the rather short lifetime of HCHO of a few hours (Arlander et al., 1995), HCHO proves to be an important indicator of local sources, e.g. biogenic emissions, biomass burning (Lipari et al., 1984; Carlier et al., 1986), and industrial activities (oxidation of non-methane hydrocarbons) over continents. In fact, while the oxidation of the relatively constant atmospheric $CH_4$ concentration also leads to a rather constant background concentration of HCHO, these additional sources cause "anomalies" in the HCHO distribution (Levi, 1971; Altshuller, 1993; Munger et al., 1995; Lee et al., 1998). Formaldehyde columns measured from space therefore provide constraints on the underlying reactive VOC emissions (e.g. Palmer et al., 2006, Stavrakou et al., 2009).

Analyzing long time series of satellite measurements provides unique opportunities for the identification and the characterization of trace gas sources on a global scale. Using our improved GOME (Global Ozone Monitoring Experiment) retrieval for formaldehyde, described in this paper, we processed the 7 year (1996 to 2002) time series of daily maps of the global formaldehyde distribution (full coverage at the equator is achieved within 3 days). From these measurements, a variety of details of the HCHO distribution can be investigated ranging from strong signals of biogenic emissions and biomass burning to rather weak signals e.g. over some industrialized regions as also shown in e.g. Thomas et al. (1998), Chance et al. (2000), or Wittrock et al. (2006). Some of the observed patterns show a very regular occurrence, while also some episodic events (e.g. caused by ENSO) are found (Spichtinger et al., 2004; Marbach et al., 2007). Longer time series can be retrieved using also the results from the SCIAMACHY instrument onboard ENVISAT (De Smedt et al., 2008).



Eyring et al. (2005) and Endresen et al. (2007) showed that shipping activity has increased considerably over the last century and currently represents a significant contribution to the global emissions of pollutants and greenhouse gases. $NO_x$ emissions due to shipping were already identified and quantified by satellite observations of $NO_2$ (Beirle et al., 2004; Richter et al., 2004, Franke et al., 2008). All studies investigated the same region between Sri Lanka and Sumatra, where the ship routes are concentrated on one single track, which is also oriented in the scanning direction (approximately east-west) of the satellite instrument. These favourable conditions ease the detection of the weak enhancements in the trace gas absorptions observed by the satellite observations.

## 2 Method: HCHO GOME retrieval

The Global Ozone Monitoring Experiment instrument (GOME, launched in 1995 onboard ERS-2) is a nadir viewing spectrometer observing the UV/visible spectral range continuously between 240 and 790 nm at a moderate spectral resolution from 0.2 to 0.4 nm (Burrows et al., 1999a). It measures the solar irradiance and the upwelling earthshine radiance. The satellite operates in a near-polar, Sun-synchronous orbit at an altitude of 780 km with a local equator crossing time at approximately 10:30. The typical ground pixel size is 40 km (along track i.e. approximately north-south) times 320 km (across-track i.e. approx. east-west). Each across-track scan is divided in three pixels (west, centre, east pixel). The coverage of the whole surface of the Earth takes three days at the equator with improving sampling towards higher latitudes (daily coverage for the polar region). A key feature of GOME is its ability to detect not only ozone but also several other chemically active atmospheric trace gases such as $NO_2$, $SO_2$, BrO, $H_2O$, OClO and HCHO by means of Differential Optical Absorption Spectroscopy DOAS (Platt, 1994; Platt and Stutz, 2008; Wagner et al., 2008). Compared to other trace gas absorptions (e.g. ozone or $NO_2$), the HCHO absorption seen by GOME is typically rather weak (of the order of 0.1% optical density OD). In addition, in the spec-

tral window of the HCHO retrieval (337–360 nm), several other trace gases ($O_3$, BrO, $NO_2$, $O_4$) show also substantial absorption features, making the retrieval a difficult task.

The HCHO signal caused by ship emissions, which is investigated in this study, is a very weak enhancement of the HCHO absorption compared to the atmospheric background absorption of HCHO. For the winter months (January to March) 1996 to 2002, the enhancement over the ship track is 2.5 time higher than the mean value measured over the central Pacific (175° E, 145° W, 20° N, 20° S) which is assumed to be a clean air sector. The unambiguous retrieval of these weak HCHO absorptions is a particular challenge. However clear spatial pattern could be recognized and an additional confidence in the significance of these absorption enhancements could be gained from the observed dependencies of the enhanced HCHO observations on cloud cover and season (described later in this paper). Because of the weakness of the HCHO signal, we performed a rather sophisticated DOAS retrieval, which is described in detail below.

First we perform an independent spectral calibration of the satellite spectra. This calibration is based on the fitting of a highly resolved solar spectrum, convoluted with the satellite slit function, to the satellite spectra. The resulting accuracy of the spectral calibration is of the order of 0.01 nm. A particular advantage is that the spectral calibration is determined directly from the measured satellite spectra. Using this spectral calibration, the trace gas cross sections HCHO (Meller et al., 2000), BrO (Wilmouth et al., 1999), $NO_2$ (Vandaele et al., 1997) are convoluted to the instruments spectral resolution. Note that for $O_3$ instead an interpolation is performed, because the used $O_3$ cross sections at 221 K and 241 K (Burrows et al., 1999) were measured with the GOME instrument itself (Burrows et al., 1999b); also $O_4$ (Greenblatt et al., 1990) is interpolated, because the spectral features of the spectrum are wider than the spectral resolution of the GOME instrument. In this way a consistent set of reference spectra is prepared (Fig. 1), which is the prerequisite to minimize the spectral interference between the HCHO absorptions with other absorbers (in particular ozone). During the spectral DOAS retrieval, all reference spectra are allowed to "shift" in wavelength to



correct for possible instrumental changes. However, "shift" of all spectra is linked to those of the Fraunhofer reference spectrum. For the Fraunhofer reference spectrum an average of several earth shine spectra selected on a daily basis over the central Pacific (175° E, 145° W, 20° N, 20° S) is used. This region is usually not affected by strong sources of HCHO and the location is symmetrical to the equator to minimize seasonal effects. Using this Fraunhofer reference spectrum instead of the direct sun measurement, overcomes the problem caused by the GOME diffuser plate (Richter and Wagner, 2001; Richter and Burrows, 2002). In addition to the absorption spectra, also a Ring spectrum is prepared; it is calculated from the daily earthshine reference (Solomon et al., 1987; Bussemer, 1993).

For the GOME observations we found that the retrieved HCHO absorptions show a systematic dependence on the viewing angle of the instrument: for the different GOME ground pixels (east, centre, west), slight, systematic offsets were found, which can not be explained by the atmospheric distribution of HCHO or the dependence of the absorption path on the viewing angle. The reason for these offsets is still not completely understood. Possible causes are the systematic dependencies of the Ring effect and the degree of polarization on the viewing angle or a calibration effect which varies with the angle of the scan mirror. While this effect is still under investigation, currently we apply a pragmatic solution to correct for these offsets: we selected two spectra (east and west pixel) over regions without significant HCHO absorption. The ratio spectrum of these two spectra is also included as an artificial "cross-section" in the fitting routine. This technique almost completely removes the artificial east-west differences. In this study, we only consider (almost) cloud free pixels, i.e., the cloud fraction (taken from the HICRU Iterative Cloud Retrieval Utilities – Grzegorski et al., 2006) being less than 20%. The result of the spectral DOAS analysis is the slant column density (SCD, the trace gas concentration along the atmospheric light paths) of HCHO. For the considered 7 years of GOME data (1996–2002) we also filter out the outliers using a median empirical SCD threshold for each orbit of $1 \times 10^{16}$ molecules per $cm^2$: in total, 1694 orbits out of about 35,000 were rejected. Using results of atmospheric radiative transfer

modeling (described more in details in the following section) and assumptions on the HCHO-profile shape we calculate Air Mass Factors (AMF) to convert the SCDs into Vertical Column Densities (VCD, the vertically integrated trace gas concentration); the AMF are defined as the ratio of SCD and VCD.

The total error of the HCHO VCD includes several components. First, a statistical component is caused by the limited signal to noise ratio of the satellite observations. From the DOAS retrieval this statistical component of the HCHO SCD is typically found to be $<4\times10^{15}$molec/cm$^2$ (standard deviation) for the GOME results (over the reference sector as well as over the ship track). Taking into account the number of individual measurements (about 200–400 per season) within a box of the ship track size (1° latitude and 9° longitude), the statistical error at the seasonal mean is thus about $3\times10^{14}$. This value is in good agreement with the scatter of the retrieved HCHO SCDs over the ship tracks (Fig. 4), which is found to be in the order of 2–$3\times10^{14}$ molec/cm$^2$. Second, the east-west offset correction (caused by the viewing angle dependency) and the conversion to vertical column densities induce additional systematic errors. The error caused by the east-west offset correction is rather small for the large number of individual observations. Especially for this study it can be neglected because we concentrate on the latitudinal variation, whereas the offset is caused by the east-west orientation of the GOME swath. The most important systematic error arises from the assumptions for the calculation of the air mass factors. For the ship track observations, we estimate this uncertainty to be about 35% (see Sect. 3).

In order to validate the GOME measurements, a comparison with MAX-DOAS (Multiaxis-DOAS) observations from the University of Bremen during the FORMAT (Formaldehyde as a tracer for oxidation in the troposphere) campaign 2002 has been made (Hak et al., 2005; Heckel et al., 2005, Wittrock, 2006). The FORMAT MAX-DOAS measurements provide ground based HCHO VCD measurements over Milano (Po valley, Italy) from 25 July to 21 August. The GOME overpass time over Milano is about 10 a.m. Thus the comparison has been made with the days of the FORMAT campaign providing 10 AM measurements as well as measurements from 9 to 11 AM in order to



check the variation. Unfortunately, due to the GOME coverage, only 10 days can be used for a comparison between MAX-DOAS and GOME VCDs. For the GOME SCDs conversion into VCDs we apply radiative transfer simulations using the fully spherical Monte-Carlo model TRACY-2 (Deutschmann and Wagner 2006; Wagner et al., 2007).

As input parameters for the Po valley region around Milano we assumed an aerosol layer with single scattering albedo of 0.97 and an asymmetry parameter of 0.68. The aerosol optical depths (AOD) are taken from the FORMAT daily measurements (Table 1). We assumed boundary layer heights of 1000, 1500 and 2000 m (Junkermann, personal communication) over Milano at the studied time. The ground albedo was set to 5% (at the wavelength used to retrieve HCHO). The AMF and VCDs for the GOME HCHO observations over Milano are shown in Table 1 and plotted in Fig. 2. The comparison with the MAX-DOAS VCD (time 10 AM) shows a good agreement. The GOME VCD also reproduce the lower values measured during the FORMAT campaign from 8 to 15 August 2002, with the lowest VCD seen in both GOME and MAX-DOAS on 12 August. The day with higher discrepancy between GOME and MAX-DOAS (6, 9 and 21 August) can be partly explained through a higher cloud fraction of the GOME over Milano (Table 1).

## 3 HCHO emissions over a ship track

According to recent studies on ocean going ship traffic (Corbett et al., 1999; Endresen et al., 2003; Eyring et al., 2007) the Atlantic ocean is the most travelled ocean of the world, but ship tracks are distributed quite homogenously. In contrast, in the Indian Ocean between Sri Lanka and Sumatra, all ship cruises follow the same narrow pathway. Due to this feature, this particular track has already been detected in $NO_2$ satellite measurements (Beirle et al., 2004; Richter et al., 2004). Over this ship track lane enhanced values are also found in our GOME HCHO data set (Fig. 3a). However, these enhanced HCHO SCDs are surrounded by enhanced values caused by other stronger HCHO sources such biomass burning or biogenic emissions originating from

the continents. In order to better identify the HCHO signal of the ship emissions we take advantage of the almost west-east orientation of the narrow ship track, which allows us to apply a high-pass filter (recursive filter with a cut off frequency of 1/1400 km) to the HCHO distribution in north-south direction. The results are shown in Fig. 3b. After applying the high-pass filter, the obtained good agreement between the trace gas patterns and the ship routes allows the assignment of ship emissions as source for the enhanced HCHO SCD.

As an additional confidence check, we investigate the dependence of the retrieved HCHO SCD on cloud cover. For that purpose we used the effective cloud fraction data retrieved with the HICRU cloud algorithm (Grzegorski et al., 2006). We found that the high-pass filtered HCHO signal is most pronounced for low cloud fractions, which indicates that the corresponding HCHO absorptions must have taken place at low altitudes. Moreover, we found that over the investigated ship track there is no correlation between the patterns found in the HCHO absorptions and those of the cloud distribution. Thus we can also exclude the possibility that the observed HCHO pattern might be an artefact caused by interference with clouds.

Similar to Beirle et al. (2004), we also investigated the seasonal variation of the enhanced HCHO signal over the ship track. For that purpose we considered the box indicated in Fig. 3b and calculated zonal means (Fig. 4). For all seasons, the HCHO distribution shows a maximum between 4° N and 9° N. However, the exact location and also the shape of the peak differs significantly for the seasons and show a strong asymmetry for summer (July–September) and winter (January–March). This is due to the fact that the ship track corridor is traversed by the Intertropical Convergence Zone (ITCZ) twice a year. As a result, the mean wind directions of summer and winter are nearly opposite. The mean meridional wind component at the surface is 6.5 m/s in summer and 4 m/s in winter (NCEP/NCAR reanalysis – Kanamitsu et al., 2002). The respective curves are broadened to the North (summer) and the South (winter), respectively, while they are quite symmetric in spring and autumn when meridional wind speeds are lower (1–2 m/s). The observed seasonal variation is an additional



independent indication that the observed weak enhancement of the HCHO absorption over ship tracks is indeed caused by ship emissions.

It is interesting to compare the HCHO observations to the $NO_2$ results of Beirle et al. (2004). Note that in that paper winter has been set from December to February and summer from June to August. The peaks of both (mean) trace gas distributions are centred around 6° N, the latitude of the ship track and similar seasonal variations are found. But although both HCHO and $NO_2$ have approximately the same lifetime (a few hours), the shifts of the winter and summer peaks extend over about twice the latitudinal distance for HCHO compared to $NO_2$. One very likely explanation is secondary formation of a large fraction of the HCHO from oxidation of VOC's (see Sect. 1), while $NO_2$ is essentially due to primary emission (NO to $NO_2$ conversion takes place in about one minute). Oxidation of VOC's emitted by ships could lead to additional HCHO formation further downwind. The larger HCHO peak width than that of $NO_2$ could also be induced from the difference in grid size used for the two trace gases, 0.5° for HCHO and 0.1° for $NO_2$.

## 4 Comparison with model results

For the estimation of emission rates from the satellite derived HCHO columns, information about the atmospheric lifetime is necessary (see also Beirle et al., 2004; Richter et al., 2004). However, as discussed above, for the observed HCHO enhancements, the estimation of the lifetime is not straight-forward and it can not directly be assessed from the shift and shape of the HCHO peaks as secondary HCHO production contributes.

Thus, we compared our observations with EMAC (ECHAM5/MESSy, atmospheric chemistry) model results in Fig. 5. The vertical columns from the model (Fig. 5c) were obtained using a horizontal resolution of T42 (corresponding to 2.8°) and a vertical resolution of 90 levels (sigma hybrid coordinates resolving the surface to 900 hPa with approximately four levels over the oceans). The model time step is 900 s and output has been archived as 5-hourly instantaneous fields (Jöckel et al., 2006). Ship emissions

are based on Eyring et al. (2005) and were released into the two lowest model levels (corresponding to 45 and 140 m, respectively). The partitioning of the NMHC-emission estimates from ships into the individual species is based on the fossil fuel specifications of von Kuhlmann et al. (2003a, b) assuming a fraction of only 0.4% being emitted directly as HCHO. Since GOME has its overpass at 10:30 local time at the equator the model data for building the monthly mean were filtered for local time between 10:00 and 11:00 a.m.

To allow the comparison with the model VCD data, the GOME SCDs have been converted into VCDs. For that purpose we apply the same radiative transfer model TRACY-2 as used and described for the validation of the GOME data (see method part). We use the following input parameters for the selected area (see Fig. 3a): for the sea salt aerosols layer (present in the first 100 m) we assumed an aerosol optical depth (AOD) of 0.2 and with single scattering albedo of 1.0 and an asymmetry parameter of 0.68, sea surface albedo of 5% (at the wavelength used to retrieve HCHO); cloud fraction of 10% (i.e. mean cloud fraction of the analyzed data with less than 20% cloud fraction) assuming the clouds to be above the HCHO layer (cloud top height=4 km, optical density=50). We assumed the HCHO concentrations to be close to the surface in the maritime boundary layer (MBL) with a height of 700 m (Beirle et al., 2004). The resulting AMF for the HCHO observations over the ocean is about 0.4. It should be noted that these AMFs are different from typical HCHO AMF over continents (close to 1) because of the different profile shapes. Using the AMF of 0.4, the peak values observed in the HCHO SCDs over the ship corridor (about $8.0\times10^{14}$molec/cm$^2$) correspond to HCHO VCDs of $2.0\times10^{15}$molec/cm$^2$. Assuming a MBL closer to the surface (200 m and AMF=0.3) or a thicker MBL (1000 m and AMF=0.6) would result in a VCD of $2.7\times10^{15}$ and $1.3\times10^{15}$molec/cm$^2$, respectively. Note that the changes of the absolute values (HCHO VCDs) do not affect the HCHO SCD ship track pattern. Finally the GOME VCDs have been binned to a 2.8° grid corresponding to the model resolution (Fig. 5a). Then the high-pass filter (with a cut off frequency adapted to the 2.8° resolution) has been applied consistently to the GOME and EMAC VCDs (Fig. 5b and



d).

Despite its resolution of 2.8 degrees, the model results from EMAC indicate an enhancement of the HCHO vertical column along the ship tracks in the Indian Ocean (Fig. 5c) and in general the shape of the HCHO distribution is similar to the one seen in the GOME data (Fig. 5a). Note that the absolute values differ because the satellite data represent the enhancement with respect to remote regions, whereas the model data show the total atmospheric columns. For the high-pass results in Fig. 5d, the obtained patterns are in good agreement with those generated through the high-pass filter of the GOME data (Fig. 5b) and underline that the HCHO enhancement can be attributed to the emissions from ship traffic. However the modelled HCHO values over the ship corridor are two times lower than for the GOME high-pass filtered data. Besides potential underestimated emissions of HCHO this difference might also be caused by the poor representation of chemical gradients in the coarse resolution of the model. The spread of $NO_x$ into the grid cell neglecting plume chemistry leads to an underestimation of OH (due to an underestimation of the reaction of NO with $HO_2$ – e.g. Song et al., 2003; Von Glasow et al., 2003). The sensitivity of OH-changes to $NO_x$-perturbations is large at low $NO_x$ conditions in particular over the tropical oceans (Lelieveld et al., 2002). Both factors may result in a lower OH -production from $NO_x$ emitted by ships which leads in turn to less efficient HCHO formation from methane in the background atmosphere. Direct emissions of HCHO are assumed to contribute only 0.4% of the NMHC-ship emission totals in the model, whereas alkenes from ship emissions contribute about 6% in the model.

We could not detect any enhanced HCHO values over other ship tracks in the GOME data, mainly for two reasons: a) the Indian Ocean track corridor is extremely narrow (in contrast to the ship tracks of Atlantic routes) leading to a distinct enhancement and b) it has the peculiarity of being oriented in the east-west direction, almost parallel to the GOME pixel. Thus, the large east-west extent of the GOME pixel does not affect the measurements.

## 5 Conclusions and outlook

In this study we present the first detection and quantification of ship HCHO-emissions from satellite observations. Although the HCHO signal is weak it could clearly be seen in the high-pass filtered satellite data. The line of enhanced HCHO in the Indian Ocean as seen in the 7-year composite of cloud screened GOME observations clearly coincides with the distinct ship track corridor from Sri Lanka to Indonesia. The effect of ship emissions on the rather pristine marine boundary layer is evident from the model simulations and it is also traceable from satellite HCHO observations.

As a result of the small absorption by HCHO, the signal in the GOME data is rather weak. However, from three additional pieces of information which can be derived from these satellite data, it becomes evident that the observed HCHO enhancement is indeed caused by the ship emissions:

a) First, the pattern coincides very well with the location of the ship tracks; also the seasonal shift of the HCHO-pattern is in agreement with the average wind directions.

b) Second, from the selection of clear and cloudy observations, it becomes clear that the bulk of the HCHO causing the signal must be close to the surface.

c) The observed HCHO pattern also agrees qualitatively and quantitatively well with result of an atmospheric chemistry transport model. The absolute magnitude of the HCHO signal is however underestimated by the model by about a factor of two. This might indicate that the used emission inventories are too low or/and that the in-plume chemistry is not well represented by the rather coarse model resolution.

In addition to the detection of the HCHO signal, the more pronounced shift in winter and summer through meridional winds (compared to $NO_2$) could indicate secondary HCHO formations.

Although the ship emissions are not a major source of HCHO globally, this study has shown that they can be detected and measured with a satellite-based instrument (GOME). GOME II (launched onboard METOP in October 2006) with improved spatial resolution might even allow the detection of further ship tracks. Ship emission have already been detected for other trace gases like $NO_2$ and other studies show an increase of the ship emissions over the last years and a further increase for the coming years is expected. However, ship emissions are one of the atmospheric pollution sources with high reduction potential. The emissions are localized and could be reduced by using more efficient engines, cleaner fuels or even new technologies.



*Acknowledgements.* The German Research Foundation (DFG) and ACCENT-TROPOSAT-2 are gratefully acknowledged for financial support. ESA is also thanked for providing the ERS-2 data. Part of this work was cofunded by the EU project QUANTIFY (contract number 003893). MV acknowledges the A.v.Humboldt foundation and the European Union (Marie Curie) for consecutive research fellowships.

The service charges for this open access publication
have been covered by the Max Planck Society.

## References

Altshuller, A. P.: Production of aldehydes as primary emissions and from secondary atmospheric reactions of alkenes and alkanes during the night and early morning hours, Atmos. Environ., 27, 21–31, 1993.

Anderson, L. G., Lanning, J. A., Barrel, R., Mityagishima, J., Jones, R. H., and Wolfe, P.: Sources and sinks of formaldehyde and acetaldehyde: An analysis of Denver's ambient concentration data, Atmos. Environ., 30, 2113–2123, 1996.

Arlander, D. W., Brüning, D., Schmidt, U., and Ehhalt, D. H.: The Tropospheric Distribution of Formaldehyde During TROPZ II, J. Atmos. Chem., 22, 251–268, 1995.

Beirle, S., Platt, U., von Glasow, R., Wenig, M., and Wagner, T.: Estimate of nitrogen oxide emissions from shipping by satellite remote sensing, Geophys. Res. Lett., 31, L18102, doi:10.1029/2004GL020312, 2004.

Burrows, J. P., Weber, M., Buchwitz, M., Rozanov, V., Ladstatter-Weissemayer, A., Richter, A., Debeek, R., Hoogen, R., Bramstedt, K., Eichmann, K.-U., Eisinger, M., and Perner, D.: The Global Ozone Monitoring Experiment (GOME): Mission concept and first scientific results, J. Atmos. Sci., 56, 151–175, 1999a.

Burrows, J. P., Dehn, A., Deters, B., Himmelmann, S., Richter, A., Voigt, S., and Orphal, J.: Atmospheric Remote-Sensing Reference Data from GOME: 2. Temperature-Dependent Absorption Cross Sections of $O_3$ in the 231–794 nm Range, J. Quant. Spectrosc. Ra., 61, 509–517, 1999b.

Bussemer, M.: Der Ring-Effekt: Ursachen und Einfluß auf die spektroskopische Messung stratosphärischer Spurenstoffe, Diploma thesis, University of Heidelberg, Heidelberg, Germany, 1993.

Carlier, P., Hannachi, H., and Mouvier, G.: The chemistry of carbonyl compounds in the atmosphere, Atmos. Environ., 20, 2079–2099, 1986.

Chance, K., Palmer, P. I., Spurr, R. J. D., Martin, R. V., Kurosu, T. P., and Jacob, D. J.: Satellite observations of formaldehyde over North America from GOME, Geophys. Res. Lett., 27, 3461–3464, 2000.

Corbett, J. J., Fischbeck, P. S., and Pandis, S. N.: Global nitrogen and sulfur inventories for oceangoing ships, J. Geophys. Res., 104, 3457–3470, 10.1029/1998JD100040, 1999.

De Smedt, I., Müller, J.-F., Stavrakou, T., van der A, R., Eskes, H., and Van Roozendael, M.: Twelve years of global observations of formaldehyde in the troposphere using GOME and SCIAMACHY sensors, Atmos. Chem. Phys., 8, 4947–4963, 2008, http://www.atmos-chem-phys.net/8/4947/2008/.

Deutschmann, T. and Wagner, T.: TRACY-II Users manual, http://joseba.mpch-mainz.mpg.de/matr/tracy_II/documentation/manual.pdf, 2006.

Endresen, Ø., Srgård, E., Sundet, J. K., Dalsren, S. B., Isaksen, I. S. A., Berglen, T. F., and Gravir, G.: Emission from international sea transportation and environmental impact, J. Geophys. Res., 108, 4560, doi:10.1029/2002JD002898, 2003.

Endresen, Ø., Srgård, E., Behrens, H. L., Brett, P. O., and Isaksen, I. S. A.: A historical reconstruction of ships' fuel consumption and emissions, J. Geophys. Res., 112, D12301, doi:10.1029/2006JD007630, 2007.

Eyring, V., Köhler, H. W., van Aardenne, J., and Lauer, A.: Emissions from international shipping: 1. The last 50 years, J. Geophys. Res., 110, D17305, doi:10.1029/2004JD005619, 2005.

Eyring, V., Stevenson, D. S., Lauer, A., Dentener, F. J., Butler, T., Collins, W. J., Ellingsen, K., Gauss, M., Hauglustaine, D. A., Isaksen, I. S. A., Lawrence, M. G., Richter, A., Rodriguez, J. M., Sanderson, M., Strahan, S. E., Sudo, K., Szopa, S., van Noije, T. P. C., and Wild, O.: Multi-model simulations of the impact of international shipping on Atmospheric Chemistry



and Climate in 2000 and 2030, Atmos. Chem. Phys., 7, 757–780, 2007, http://www.atmos-chem-phys.net/7/757/2007/.

Franke, K., Richter, A., Bovensmann, H., Eyring, V., Jöckel, P., and Burrows, J. P.: Ship emitted $NO_2$ in the Indian Ocean: comparison of model results with satellite data, Atmos. Chem. Phys. Discuss., 8, 15997–16025, 2008, http://www.atmos-chem-phys-discuss.net/8/15997/2008/.

Greenblatt, G. D., Orlando, J. J., Burkholder, J. B., and Ravishankara, A. R.: Absorption measurements of oxygen between 330 and 1140 nm, J. Geophys. Res., 95, 18577–18582, 1990.

Grzegorski, M., Wenig, M., Platt, U., Stammes, P., Fournier, N., and Wagner, T.: The Heidelberg iterative cloud retrieval utilities (HICRU) and its application to GOME data, Atmos. Chem. Phys., 6, 4461–4476, 2006, http://www.atmos-chem-phys.net/6/4461/2006/.

Hak, C., Pundt, I., Trick, S., Kern, C., Platt, U., Dommen, J., Ordóñez, C., Prévôt, A. S. H., Junkermann, W., Astorga-Lloréns, C., Larsen, B. R., Mellqvist, J., Strandberg, A., Yu, Y., Galle, B., Kleffmann, J., Lörzer, J. C., Braathen, G. O., and Volkamer, R.: Intercomparison of four different in-situ techniques for ambient formaldehyde measurements in urban air, Atmos. Chem. Phys., 5, 2881–2900, 2005, http://www.atmos-chem-phys.net/5/2881/2005/.

Heckel, A., Richter, A., Tarsu, T., Wittrock, F., Hak, C., Pundt, I., Junkermann, W., and Burrows, J. P.: MAX-DOAS measurements of formaldehyde in the Po-Valley, Atmos. Chem. Phys., 5, 909–918, 2005, http://www.atmos-chem-phys.net/5/909/2005/.

Jöckel, P., Tost, H., Pozzer, A., Brühl, C., Buchholz, J., Ganzeveld, L., Hoor, P., Kerkweg, A., Lawrence, M. G., Sander, R., Steil, B., Stiller, G., Tanarhte, M., Taraborrelli, D., van Aardenne, J., and Lelieveld, J.: The atmospheric chemistry general circulation model ECHAM5/MESSy1: consistent simulation of ozone from the surface to the mesosphere, Atmos. Chem. Phys., 6, 5067–5104, 2006, http://www.atmos-chem-phys.net/6/5067/2006/.

Kanamitsu, M. et al.: NCEP-DEO AMIP-II Reanalysis (R-2), Bul. Atmos. Met. Soc. 83, 1631–1643, 2002.

Lee, Y.-N. et al.: Atmospheric chemistry and distribution of formaldehyde and several multioxygenated carbonyl compounds during the 1995 Nashville/Middle Tennessee Ozone Study, J. Geophys. Res., 103, 22449–22462, 1998.

Lelieveld, J., Peters, W., Dentener, F., and Krol, M.: Stability of tropospheric hydroxyl chemistry, J. Geophys. Res., 107(D23), 4715, doi:10.1029/2002JD002272, 2002.
Levi, H.: Normal atmosphere: Large radical and formaldehyde concentrations predicted, Sciences, 173, 141–143, 1971.
Lipari, F., Dasch, J. M., and Scuggs, W. F.: Aldehyde emissions from wood-burning fireplaces, Environ. Sci. Technol., 18, 326–330, 1984.
Marbach, T., Beirle, S., Frankenberg, C., Platt, U., and Wagner, T.: Identification of tropospheric trace gas sources: synergistic use of HCHO and other satellite observations, ESA publication SP-636, ISBN 92-9291-200-1, ESA Communication Production Office, Noordwijk, 2007
Meller, R. and Moortgat, G. K.: Temperature dependence of the absorption cross sections of formaldehyde between 223 and 323 K in the wavelenght range 225–375 nm, J. Geophys. Res., 105, 7089–7101, 2000.
Munger, J. W., Jacob, D. J., Daube, B. C., Horowitz, L. W., Keene, W. C., Heikes, B. G.: Formaldehyde, glyoxal. and methylglyoxal at a rural mountain site in central Virginia, J. Geophys. Res., 100, 9325–9334, 1995.
Palmer, P. I., Abbot, D. S., Fu, T-M., Jacob, D. J., Chance, K., Kurosu, T., Guenther, A., Wiedinmyer, C., Stanton, J., Pilling, M., Pressley, S., Lamb, B., and Sumner, A. L.: Quantifying the seasonal and interannual variability of North American isoprene emissions using satellite observations of formaldehyde column, J. Geophys. Res., 111, D12315, doi:10.1029/2005JD006689, 2006.
Platt, U.: "Differential optical absorption spectroscopy (DOAS)", in Air Monitoring by Spectroscopic Techniques, Chem. Anal. Ser., 127, 27–84, 1994.
Platt, U. and Stutz, J.: Differential Optical Absorption Spectroscopy Principles and Applications, in: Series: Physics of Earth and Space Environments, ISBN: 978-3-540-21193-8, Springer, Berlin, Germany, 597 p., 2008.
Richter, A. and Wagner, T.: Diffuser Plate Spectral Structures and their Influence on GOME Slant Columns, Technical Note, 2001.
Richter, A. and Burrows, J.: Retrieval of Tropospheric $NO_2$ from GOME Measurements, Adv. Space Res., 29(11), 1673–1683, 2002.
Richter, A., Eyring, V., Burrows, J. P., Bovensmann, H., Lauer, A., Sierk, B., and Crutzen, P. J.: Satellite measurements of $NO_2$ from international shipping emissions, Geophys. Res. Lett., 31, L23110, doi:10.1029/2004GL020822, 2004.
Solomon, S., Schmeltekopf, A. L., and Sanders, R. W.: On the interpretation of zenith sky



absorption measurements, J. Geophys. Res., 92, 8311–8319, 1987.
Song, C. H., Chen, G., Hanna, S. R., Crawford, J., and Davis, D. D.: Dispersion and chemical evolution of ship plumes in the marine boundary layer: Investigation of $O_3/NO_y/HO_x$ chemistry version, J. Geophys. Res., 108, 4143, doi:10.1029/2002JD002216, 2003.
Stavrakou, T., Müller, J.-F., De Smedt, I., Van Roozendael, M., van der Werf, G. R., Giglio, L., and Guenther, A.: Evaluating the performance of pyrogenic and biogenic emission inventories against one decade of space-based formaldehyde columns, Atmos. Chem. Phys., 9, 1037–1060, 2009,
http://www.atmos-chem-phys.net/9/1037/2009/.
Spichtinger, N., Damoah, R., Eckhardt, S., Forster, C., James, P., Beirle, S., Marbach, T., Wagner, T., Novelli, P. C., and Stohl, A.: Boreal forest fires in 1997 and 1998: a seasonal comparison using transport model simulations and measurement data, Atmos. Chem. Phys., 4, 1857–1868, 2004,
http://www.atmos-chem-phys.net/4/1857/2004/.
Thomas, W., Hegels, E., Slijkhuis, S., Spurr, R., and Chance, K.: Detection of biomass burning combustion products in Southeast Asia from backscatter data taken by the GOME spectrometer, Geophys. Res. Lett., 25, 1317–1320, 1998.
Vandaele, A. C., Hermans, C., Simon, P. C., Carleer, M., Colin, R., Fally, S., Mérienne, M.-F., Jenouvrier, A., and Coquart, B.: Measurements of the NO2 Absorption Cross-section from 42000 $cm^{-1}$ to 10000 $cm^{-1}$ (238–1000 nm) at 220 K and 294 K, J. Quant. Spectrosc. Radiat. Transfer, 59, 171–184, 1997.
von Glasow, R., Lawrence, M. G., Sander, R., and Crutzen, P. J.: Modeling the chemical effects of ship exhaust in the cloud-free marine boundary layer, Atmos. Chem. Phys., 3, 233–250, 2003,
http://www.atmos-chem-phys.net/3/233/2003/.
von Kuhlmann, R., Lawrence, M. G., Crutzen, P., and Rasch, P.: A model for studies of tropospheric ozone and nonmethane hydrocarbons: Model description and ozone results, J. Geophys. Res., 108, 4294, doi:10.1029/2002JD002893, 2003a.
von Kuhlmann, R., Lawrence, M. G., Crutzen, P., and Rasch, P.: A model for studies of tropospheric ozone and nonmethane hydrocarbons: Model evaluation of ozone related species, J. Geophys. Res., 108, 4729, doi:10.1029/2002JD003348, 2003b.
Wagner, T., Burrows, J. P., Deutschmann, T., Dix, B., von Friedeburg, C., Frieß, U., Hendrick, F., Heue, K.-P., Irie, H., Iwabuchi, H., Kanaya, Y., Keller, J., McLinden, C. A., Oetjen, H.,

Palazzi, E., Petritoli, A., Platt, U., Postylyakov, O., Pukite, J., Richter, A., van Roozendael, M., Rozanov, A., Rozanov, V., Sinreich, R., Sanghavi, S., and Wittrock, F.: Comparison of box-air-mass-factors and radiances for Multiple-Axis Differential Optical Absorption Spectroscopy (MAX-DOAS) geometries calculated from different UV/visible radiative transfer models, Atmos. Chem. Phys., 7, 1809–1833, 2007, http://www.atmos-chem-phys.net/7/1809/2007/.

Wagner, T., Beirle, S., Deutschmann, T., Eigemeier, E., Frankenberg, C., Grzegorski, M., Liu, C., Marbach, T., Platt, U., and Penning de Vries, M.: Monitoring of atmospheric trace gases, clouds, aerosols and surface properties from UV/vis/NIR satellite instruments, J. Opt. A: Pure Appl. Opt., 10(10), 104019, doi:10.1088/1464-4258/10/10/1040192008, 2008.

Wilmouth, D. M., Hanisco, T. F., Donahue, N. M., and Anderson, J. G.: Fourier transfor ultraviolet spectroscopy of the A2P3/2 X2P3/2 transition of BrO, J. Phys. Chem. A., 103, 8935–8945, 1999.

Wittrock, F.: The retrieval of oxygenated volatile organic compounds by remote sensing techniques, Ph.D. thesis, Institute of Environmental Physics, University of Bremen, Bremen, http://nbn-resolving.de/urn:nbn:de:gbv:46-diss000104818, 2006.

Wittrock, F., Richter, A., Oetjen, H., Burrows, J. P., Kanakidou, M., Myriokefalitakis, S., Volkamer, R., Beirle, S., Platt, U., and Wagner, T.: Simultaneous global observations of glyoxal and formaldehyde from space, Geophys. Res. Lett., 33, L16804, doi:10.1029/2006GL026310, 2006.



**Table 1.** GOME VCD results using the following aerosols properties: single scattering albedo of 0.97, an asymmetry parameter of 0.68. The surface albedo was set to 5%. The aerosol optical depths (AOD) have been measured from the ground during FORMAT campaign. The GOME VCD are calculated for the range of boundary layer height (BL) occurring over Milano during the studied time. The GOME VCDs are also plotted with the MAX-DOAS VCD in Fig. 2.

| Date | VCD MAX-DOAS $\times 10^{16}$ molec/cm$^2$ Time: 10:00 a.m. | VCD GOME $\times 10^{16}$ molec/cm$^2$ *(AMF)* BL: 1000 m | VCD GOME $\times 10^{16}$ molec/cm$^2$ *(AMF)* BL: 1500 m | VCD GOME $\times 10^{16}$ molec/cm$^2$ *(AMF)* BL: 2000 m | AOD | Cloud Fraction HICRU |
|---|---|---|---|---|---|---|
| 27 Jul 2002 | 1.20 | 1.40 *(0.60)* | 1.19 *(0.71)* | 1.03 *(0.82)* | 0.370 | 0.02 |
| 30 Jul 2002 | 1.14 | 0.92 *(0.51)* | 0.77 *(0.61)* | 0.67 *(0.70)* | 0.255 | 0.05 |
| 03 Aug 2002 | 1.14 | 1.84 *(0.54)* | 1.53 *(0.65)* | 1.33 *(0.75)* | 0.716 | 0.10 |
| 06 Aug 2002 | 1.12 | 1.91 *(0.24)* | 1.54 *(0.30)* | 1.32 *(0.35)* | 0.716 | 0.41 |
| 08 Aug 2002 | 0.68 | 0.32 *(0.64)* | 0.27 *(0.76)* | 0.24 *(0.88)* | 0.543 | 0.02 |
| 09 Aug 2002 | 0.69 | 1.32 *(0.10)* | 1.11 *(0.12)* | 0.95 *(0.14)* | 0.139 | 0.59 |
| 12 Aug 2002 | 0.04 | 0.08 *(0.82)* | 0.07 *(0.94)* | 0.06 *(1.07)* | 1.060 | 0.00 |
| 15 Aug 2002 | 0.83 | 0.67 *(0.54)* | 0.57 *(0.64)* | 0.49 *(0.74)* | 0.139 | 0.01 |
| 18 Aug 2002 | 1.25 | 1.51 *(0.75)* | 1.31 *(0.86)* | 1.16 *(0.98)* | 1.060 | 0.03 |
| 21 Aug 2002 | 1.28 | 3.15 *(0.54)* | 2.67 *(0.64)* | 2.33 *(0.73)* | 1.060 | 0.15 |

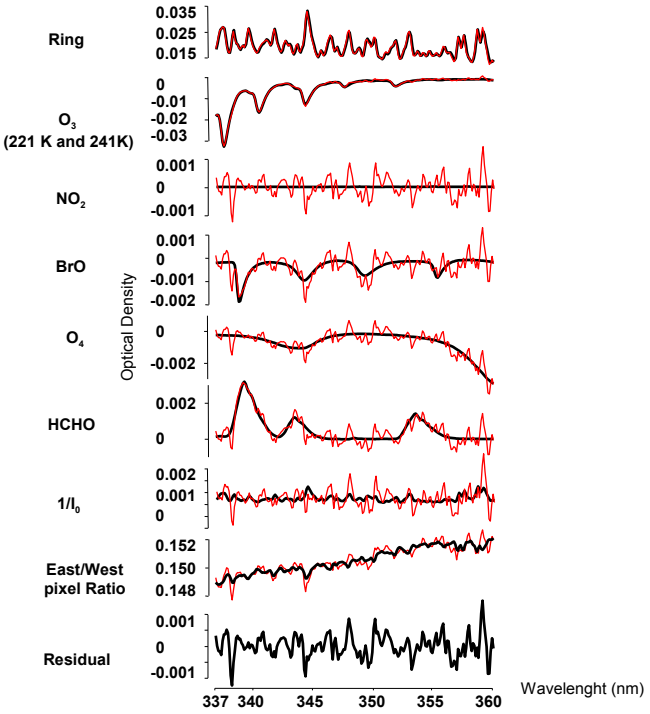


**Fig. 1.** Example of the HCHO DOAS retrieval. The displayed retrieval was done for a GOME pixel from 9 Sep 1997 over the Borneo island (GOME Orbit 70927023, Lat.: −0.38°, Long.: 113.66°, SZA: 20.5°). During that time strong biomass burning took place on the island inducing an enhanced HCHO signal. The black lines show the fitted cross section while the retrieved spectral signature is shown in red.



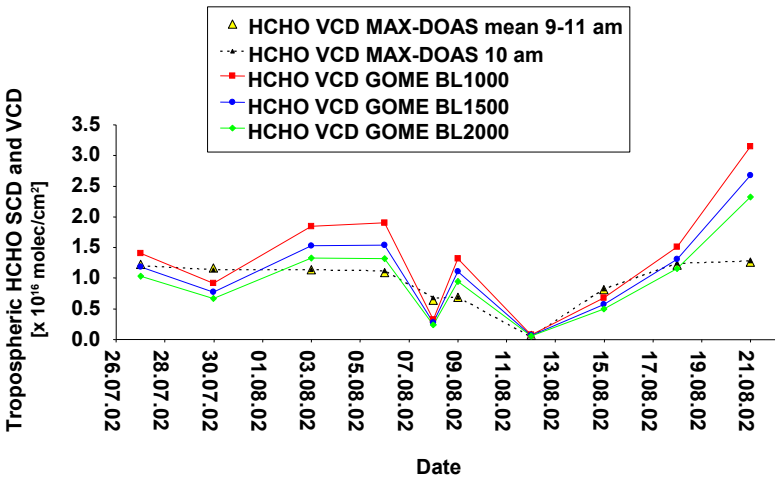


**Fig. 2.** GOME VCD for typical boundary layer heights (BL) of 1000, 1500, and 2000 m expected over Milano at the time studied. The comparison with the MAX-DOAS VCD (Heckel et al., 2005) of the FORMAT campaign (at 10:00 a.m.) shows a good agreement. Also the low values measured around 12 August 2002 are well reproduced in the GOME results. The days with higher discrepancy can be partly explained through a higher cloud fraction (values in Table 1). The MAX-DOAS VCD (time 9:00–11:00 a.m. mean) are also displayed for information on temporal variability.

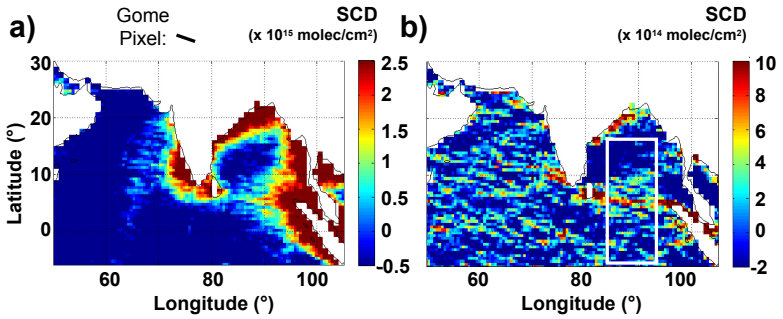


**Fig. 3.** HCHO distribution over the Indian Ocean (land masses are masked out). **(a)** GOME SCDs during winters (January to March) 1996–2002 with cloud fractions below 20% are averaged. The ship track is visible from Sri Lanka until about half the distance to Sumatra. For illustration, size and orientation of a single GOME pixel is displayed above panel a. **(b)** High-pass filtered (along latitudinal component) HCHO SCDs for cloud fractions below 20%. The narrow ship track between Sri Lanka and Sumatra is now clearly visible. The box (84°–93° E, 5°S–18° N) indicates the data used for the cross section calculation (see Fig. 4).



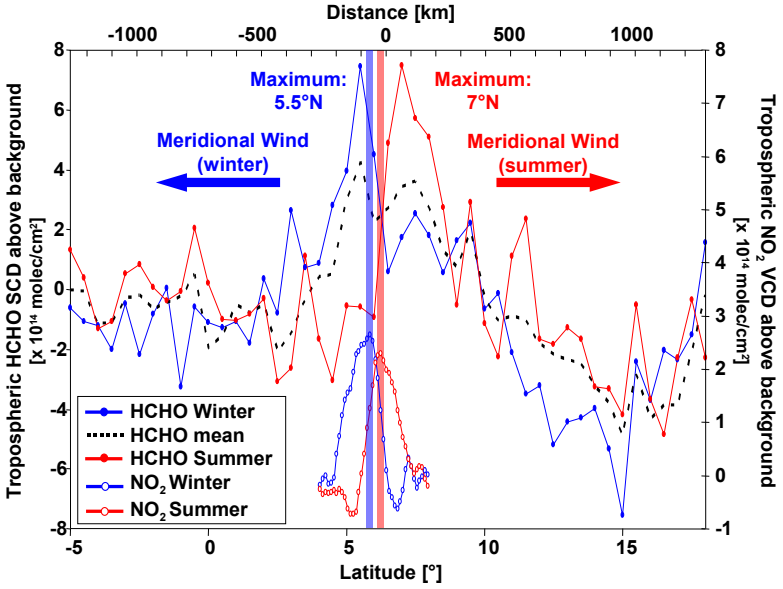


**Fig. 4.** High-pass filtered tropospheric HCHO SCDs, zonally averaged over the box in Fig. 3b, as function of latitude (below) with an additional km-scale (above). For all seasons, a maximum at the ship track position (between 4° N and 9° N) can be seen. The graphs for winter (January to March) and summer (July to September) are asymmetric due to strong meridional winds (see text), indicated by the arrows. The seasonal HCHO shift is larger in winter and summer compared to the results for $NO_2$ of Beirle et al. (2004). Note that in that paper winter has been set from December to February and summer from June to August.

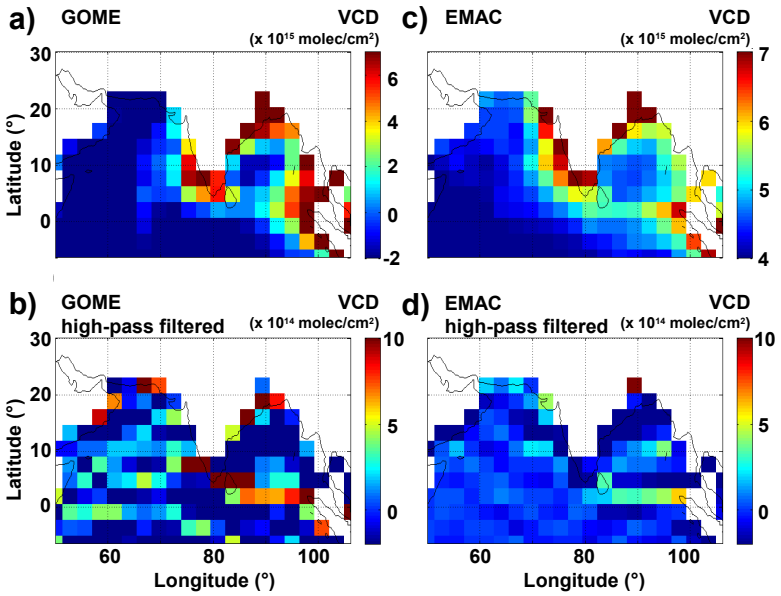


**Fig. 5.** **(a)** GOME VCDs of winters (January to March) 1996–2002 with cloud fractions below 20% (interpolated to the 2.8° model resolution). **(b)** High-pass filtered (along latitudinal component) GOME HCHO VCDs. **(c)** Model results of the mean HCHO VCDs for winter (January to March) 1997–2002, integrated up to 50 hPa (using EMAC local time between 10:00–11:00 a.m.). **(d)** EMAC model results, applying the same high-pass filter as for the GOME data **(b)**, display enhanced HCHO VCDs over the ship corridor.